

# The steric component of sea level rise associated with enhanced greenhouse warming: a model study

Kirk Bryan

Program in Atmospheric and Oceanic Sciences, Sayre Hall, Princeton University, Princeton, NJ 08544 USA

Received: 20 March 1995 / Accepted: 14 August 1995

**Abstract.** Climate change due to enhanced greenhouse warming has been calculated using the coupled GFDL general circulation model of the atmosphere and ocean. The results of the model for a sustained increase of atmospheric carbon dioxide of 1% per year over a century indicate a marked warming of the upper ocean. Results of the model are used to study the rise in sea level caused by increase in ocean temperatures and associated changes in ocean circulation. Neglecting possible contributions due to changes in the volume of polar ice sheets and mountain glaciers, the model predicts an average rise in sea level of approximately  $15 \pm 5$  cm by the time atmospheric carbon dioxide doubles. Heating anomalies are greatest in subpolar latitudes. This effect leads to a weakening of the ocean thermohaline circulation. Changes in thermohaline circulation redistribute heat within the ocean from high latitudes toward the equator, and cause a more uniform sea level rise than would occur otherwise.

## 1 Introduction

There are several components to long-term, secular changes in global sea level. The amplitude of these secular changes appears to be roughly proportional to the length of the time scale. The largest component is associated with changes in the geometry of ocean basins due to movements of the tectonic plates. An example is the flooding of the continents during the Mesozoic period, which ended about 80 million years ago. Another component, which has been particularly important in the Quaternary age of the last few million years, is associated with an exchange of large volumes of water stored in ice sheets between the land and the sea. On a decadal time scale, the melting of mountain glaciers, changes in ocean circulation and the thermal expansion of ocean waters due to global changes in ocean temperature are important. While these decadal time scale components are relatively small, they are of special interest. A net heating or cooling of the

ocean is a robust measure of changing global climate. Assuming that future measurements will provide a precise measure of the melting of land ice, a rise in sea level may be considered an important tool for detecting significant climate change due to both natural climate variability or an enhanced greenhouse warming associated with anthropogenic gases.

Considerable controversy exists regarding the interpretation of historical sea level data. A rather small number of long-term tidal records exist, and they are mainly for sites in the Northern Hemisphere. The sea level records must be corrected for local elevation changes due to purely geologic processes. The assumption is usually made that the rise in sea level is globally uniform, neglecting local effects due to long term changes in ocean circulation. The model calculations of this study show that this assumption is not really justified. Gornitz et al. (1982) and Gornitz and Lebedeff (1987) concluded from tide gauge data that global sea level has been rising at a rate of about 12 cm/century. Meier (1984) determined that large ice sheets have not changed significantly over the past century, but small mountain glaciers have been shrinking at a rate which would have contributed  $5 \pm 3$  cm/century to global sea level. Peltier and Tushingham (1989) have made more detailed corrections for isostatic adjustments of the continents due to glacial rebound from the last ice age. They estimated a slightly higher sea level rise of about  $24 \pm 9$  cm/century.

This study is concerned with future sea level rise due to thermal expansion of the ocean associated with global warming. A recent calculation of enhanced greenhouse warming using the GFDL (Geophysical Fluid Dynamics Laboratory) coupled atmosphere-ocean model (Stouffer et al. 1989; Manabe et al. 1991) was repeated to correct a minor error in the ocean component of the model that caused a distortion of the barotropic flow in the Arctic Ocean. Although this error caused a local distortion of the sea level in the Greenland and Norwegian sea area of the model, the repeat calculation demonstrated that it did not have any appreciable effect on fields elsewhere in the model

during the first century of integration. To be consistent, however, all results reported in this study will refer to the analysis of the repeat run unless otherwise stated.

The coupled model allows the exploration of several aspects of the sea level rise problem that have been neglected in previous modeling studies (see Warwick and Oerlemans 1990, for a recent review). The coupled model includes the large-scale air-sea interaction associated with a non-equilibrium response of climate to increasing greenhouse gases. Although the resolution of the ocean circulation model is inadequate to resolve many of the observed features of the ocean circulation, the model contains realistic water mass formation processes which have been tested in simulations of transient geochemical tracers. In a pioneering study of this problem Mikolajewicz et al. (1990) used a comparable ocean circulation model to examine sea level rise, but the ocean model was driven by specified upper boundary conditions which were obtained from an equilibrium response calculation of greenhouse warming made with an atmospheric model alone. As indicated in a review by the Intergovernmental Panel on Climate Change (IPCC 1990) the patterns of sea surface temperature response to greenhouse warming from atmospheric models coupled to simple mixed layer models of the ocean are significantly different from the transient response calculated in more complete atmosphere-ocean models. While it turns out that there are no real differences in the prediction of globally averaged steric sea level rise between the Mikolajewicz et al. (1990) study and the present study, there are important differences in spatial distribution. This has also been confirmed in a series of recent studies of fully coupled models (Cubasch et al. 1992, 1994, 1995; Gregory 1993). Allowing for biases due to experimental design, there is remarkable agreement among these studies in the projected globally averaged rise in sea level due to enhanced greenhouse warming. Results will be compared to the present study in the final discussion.

An important aspect of the Manabe et al. (1991) enhanced greenhouse warming simulation is that the coupled model is carefully initialized to a nearly steady state with respect to the global heat balance. The simulation does contain a climate "drift" in global sea level, but it will be shown that it is much smaller than that due to enhanced greenhouse warming. For a more complete explanation of the initialization of the coupled model, the reader is referred to Manabe et al. (1991). Only a brief account is given here. The coupled model is initialized as follows; first, the atmospheric model is integrated to a balanced state with a specified sea surface temperature, which varies with season of the year and position, according to climatological data. Next, the fluxes of momentum, heat and net moisture calculated from the atmospheric model are applied to the ocean model with the additional constraint that the surface temperature and salinity are not allowed to depart by more than small amounts from observed values. An extended calculation is carried out and conver-

gence to equilibrium in the ocean model is accelerated using methods outlined in Bryan (1984). Due to model biases, the model fluxes obtained in the first two stages of the calculation are not in agreement. The differences between the heat and moisture fluxes obtained in the first two stages of the calculation are used as fixed flux adjustments in the coupled model to minimize climate drift (Sausen et al., 1988; Manabe and Stouffer 1988). In the coupled model, the atmospheric model supplies fluxes of momentum, and adjusted fluxes of heat and net moisture to the ocean model. In turn, the ocean model supplies a prediction of the sea surface temperature to the atmospheric model.

The use of fixed water and heat flux adjustments in a coupled model has been severely criticized. However, this strategy was merely the recognition of the fact that ocean and atmospheric models were too crude at that stage to produce a realistic simulation of the Earth's climate when coupled together unless some of the model bias was removed. Higher resolution in the same coupled general circulation model substantially reduces required flux adjustments (R. J. Stouffer, personal communication).

An important feature of the model solution is the gradual loss of the ocean circulation intensity as the enhanced greenhouse warming proceeds. In order to understand this process, another, much simpler model has been developed in a companion study by Hsieh and Bryan (1996) which allows global sea level rise to be studied in a much simpler context. Massive redistribution of buoyancy within the ocean is required to produce the global sea level changes predicted by the model. The results of the simpler model provide some insights on the mechanism and time scale of this buoyancy redistribution process that depend on planetary waves.

This study contains a brief description of the globally averaged rise in sea level due to density changes in response to enhanced greenhouse warming in the coupled, atmosphere-ocean model. Changes in dynamic topography are shown to provide a picture of differences in regional sea level change. Finally some analysis is presented to explain the redistribution of density within the ocean from enhanced buoyancy source regions to other parts of the ocean.

## 2 Simulating enhanced greenhouse warming

Three different numerical experiments were carried out, starting from the same, initially balanced state (Manabe et al. 1991). In the main experiment atmospheric carbon dioxide was increased at the rate of 1%/year for 100 years. In another experiment atmospheric carbon dioxide was decreased 1%/y, and a third experiment was a control run in which the atmospheric carbon dioxide level was kept constant. The first experiment approximately corresponds to the Intergovernmental Panel on Climate Change (IPCC 1990) "business as usual" scenario. Previously, estimates of global patterns of enhanced greenhouse warming were

usually based on equilibrium response calculations. Although it has been recognized for a long time that the uptake of heat by the oceans would greatly delay the onset of global warming, it was felt that the pattern of response would be similar to that expected from equilibrium models with a globally uniform reduction in amplitude. Stouffer et al. (1989), however, confirmed the results of an early calculation (Bryan et al. 1988) that the non-equilibrium response of a global, ocean-atmosphere system may have very different patterns than predicted in the simpler, equilibrium response calculations. The most significant difference is in the Southern Hemisphere. The very effective vertical exchange between the surface and the deep ocean in the vicinity of the Circumpolar Current and in the northern North Atlantic gives much less warming at the ocean surface in these areas. Polar amplification of warming is present in the Northern Hemisphere over land areas, but is nearly absent in the Southern hemisphere.

The asymmetry between the hemispheres can be seen in the zonally averaged temperature change shown in Fig. 1a. This pattern corresponds to an average over years 70–80 of the main experiment section. As mentioned in the introduction, all results will refer to the recently repeated greenhouse warming run unless otherwise stated. Over the period of years 70–80, carbon dioxide in the atmospheric model has increased to twice the normal level. In the Northern Hemisphere temperature changes of  $0.5^{\circ}\text{C}$  penetrate to 800 m at  $60^{\circ}\text{N}$ . At the corresponding latitude in the Southern Hemisphere temperature changes are less than  $0.5^{\circ}\text{C}$  at all levels. A slight cooling is actually present in surface waters very close to the Antarctic Continent. It should be noted that the ocean areas represented by the zonally averaged changes shown in Fig. 1a are vastly different in the two hemispheres. In subpolar latitudes of the Northern Hemisphere the ocean is only present in a narrow span of longitudes, principally in the North Atlantic. In the Southern Hemisphere, ocean is present around the entire globe in the latitudes of the Drake Passage.

The equivalent change in ocean salinity is shown in Fig. 1b. The main feature of the salinity change is a tendency for salinity to increase in low and middle latitudes, and to decrease in polar regions. The freshening of the Arctic Ocean is particularly strong with a drop in surface salinity of 1 part/thousand. As pointed out by Manabe et al. (1991) two factors are responsible for the salinity change. One factor is an increased intensity of the hydrologic cycle. This involves increased evaporation from the ocean in low latitudes and greater poleward transport of water in the atmosphere in both hemispheres. The other factor, which is particularly important in the Arctic is a change in the intensity of the thermohaline circulation. The effect of a reduction of overturning in the Atlantic by 30% is to isolate the Arctic Ocean and prevent mixing with the much saltier waters of the subtropical Atlantic. It should be noted that only net melting of land ice masses and sea ice will change the average salinity of the ocean. Although the

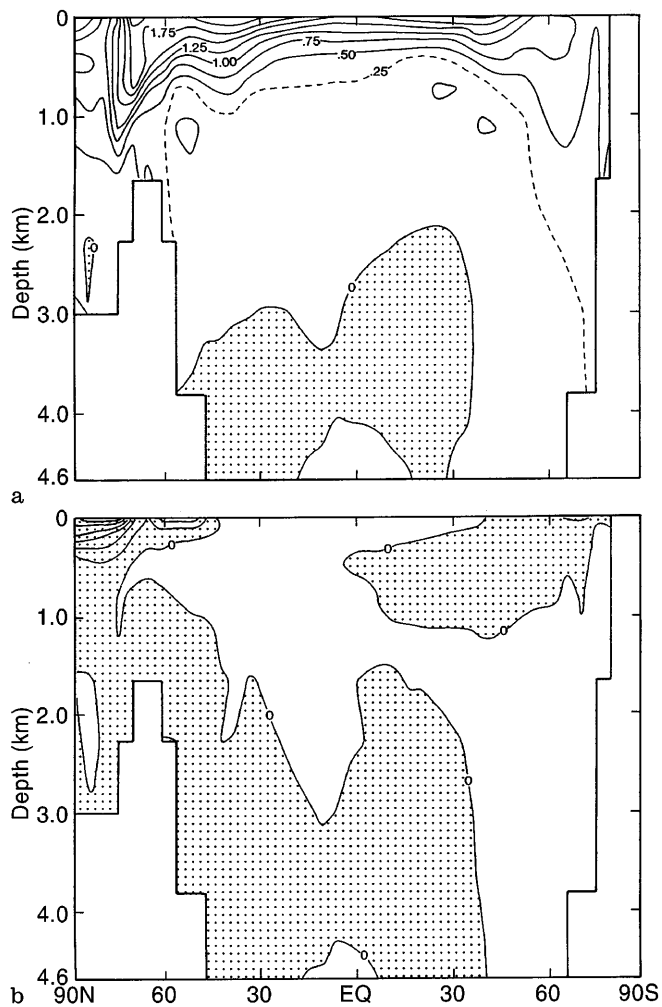


**Fig. 1.** **a** The zonally averaged temperature change in  $^{\circ}\text{C}$  for the coupled model at the time of atmospheric carbon dioxide doubling. **b** The corresponding change for salinity. The response is essentially unchanged from that given by Manabe et al. (1991). The contour interval is 0.1 p.s.u.

effects of salinity on ocean volume are very complex due to the complicated equation of state for sea water, one would anticipate that changes in salinity distribution in the ocean play a role in the regional distribution of sea level rise rather than the global average.

To provide some insight on global heat uptake by the oceans, let us consider a simple linear scaling which is based on previous numerical experiments. The scaling depends on the ocean circulation remaining essentially the same, while the waters of the World Ocean slowly gain heat. Such an argument is clearly not valid for scenarios of greatly enhanced greenhouse warming sustained over several centuries. However, it should be useful for understanding the range of possible climatic changes that are likely to take place over the next 50–100 y.

The temperature rise of the lower atmosphere due to an enhanced greenhouse effect is found to be proportional to the logarithm of increased greenhouse gases (Manabe et al. 1991). As a first approximation

we assume that an exponential increase of atmospheric greenhouse gases leads to a nearly linear increase in global mean surface temperature. If  $\langle SST \rangle$  is the globally average sea surface temperature, we would expect that,

$$\Delta \langle SST \rangle \propto t \quad (1)$$

where  $t$  is the time elapsed since the beginning of the experiment.  $\Delta \langle SST \rangle$  is the departure of the global mean sea surface from climate equilibrium. A linear increase of sea surface temperature with time is consistent with the results reported by Manabe et al. (1991). Bryan et al. (1984) show that a small perturbation of heat, or a neutrally buoyant tracer spreads downward from the surface following the same scaling laws as a simple diffusive model (Crank 1975), although the processes are much more complex. This implies for a uniformly conducting medium that the flux scales as the reciprocal of the square root of  $t$  in response to a step function increase of  $\langle SST \rangle$  at the surface. The total excess heat gained by the ocean is then proportional to the integral of the flux,

$$\text{Total Heat} \propto \int \Delta \langle SST \rangle t^{-1/2} dt \propto t^{3/2} \quad (2)$$

The same  $t^{3/2}$  law for total heat uptake may be found in the exact solution for a semi-infinite, uniformly conducting medium, if the temperature at the upper boundary increases linearly with respect to time (Crank 1975, p. 33).

Figure 2 shows the globally averaged steric rise in sea level (that component due to density changes) predicted by the model and the change in globally averaged ocean temperature. In the model itself volume is conserved so that the globally averaged sea level rise must be computed inferred from the globally averaged density change. For a formal justification of the procedure the reader is referred to a recent note by Greatbatch (1994). Volume averaged temperature changes and global sea level rise in a somewhat parallel fashion, but due to complex salinity and pressure effects they are not exactly proportional. Heat storage increases at a faster rate than sea level rise. One mechanism contributing to this is the fact that as excess heat penetrates to greater and greater depths the temperature of the water being heated is lower. At lower temperatures the thermal expansion coefficient of water decreases. Thus as warming extends to greater depths the ratio of volume increase to heat gain becomes less. Note that warming takes place at a faster rate than predicted by the simple, semi-infinite diffusion model. This should not be surprising considering the great difference in complexity of the ocean circulation model and a simple diffusion model.

From Fig. 2 we see that the average increase of temperature of the entire ocean is about  $0.1^\circ\text{C}$  between year 50 and year 70. Taking the average depth of the ocean to be 4 km, we find that the ocean has been heated by approximately  $1.6 \times 10^9$  Joules/m<sup>2</sup> over a 20 year period. This amounts to a little over  $3 \text{ W/m}^2$ , which is well below the detection level of standard marine meteorological measurements (Dobson et al.

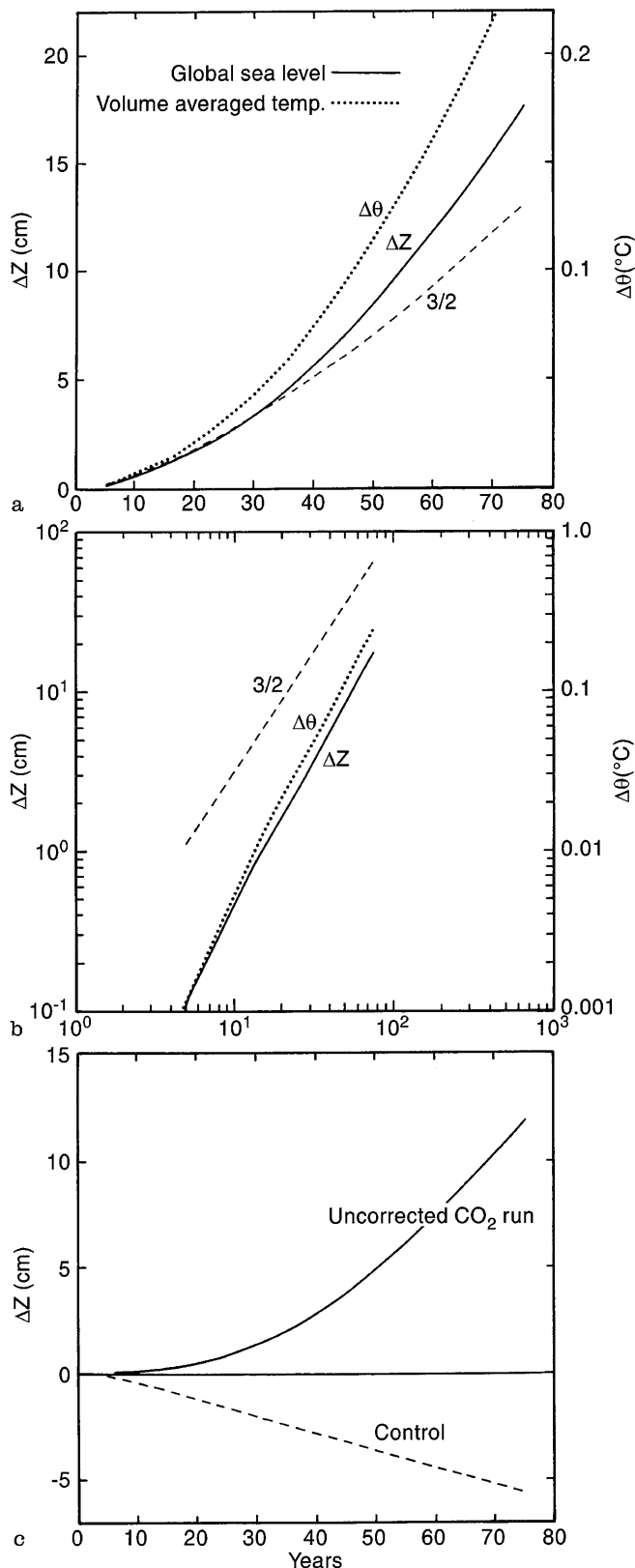


**Fig. 2.** **a** The increase of decadal averaged values of global sea level in centimeters (*solid curve*). The corresponding change in temperature in  $^\circ\text{C}$  averaged over the volume of the World Ocean (*dotted curve*). The *dashed line* shows a slope equivalent to  $t^{3/2}$ . **b** Same as **a** with logarithmic coordinates. **c** The uncorrected increase in decadal averaged sea level and the drift downward of sea level in the control run

1982). Figure 2 illustrates the usefulness of new methods for making measurements of the heat content of the ocean for monitoring climate change (Munk and Forbes 1989).

A thousand year control run has been carried out and the results for the first 600 years are reported in a recent paper by Delworth et al. (1993). In spite of the flux adjustment and other procedures used to initialize the model, some climate drift remains. Very little change takes place in sea surface temperature, but a slow cooling takes place at deeper levels of the model ocean. Results for sea level change in the control run are shown in Fig. 2c. Over the first 70 years the sea level drops about 3 cm in the control run. Note that the rise in sea level is only 12 cm over the same period for the increasing carbon dioxide run, but corrected for climate drift it becomes  $15 \pm 5$  cm as shown in Fig. 2a, b. Note that the "climate drift" in global mean sea level is taken as a measure of uncertainty.

### 3 Geographical distribution of the sea level rise

The most useful aspect of using a general circulation model of the ocean to estimate sea level rise is a pre-

diction of the spatial distribution of the sea level rise. Unfortunately sea level is not explicitly predicted by the ocean model, which uses a rigid-lid approximation to filter out fast-moving external gravity waves. We have used a traditional method to estimate sea level patterns, which is to assume that surface pressure patterns are entirely compensated by density changes within the upper part of the water column. The dynamic topography is defined as the thickness between two pressure levels. In Fig. 3 we show thickness changes between zero and 1130 decibars, where a decibar approximately corresponds to the pressure difference caused by a meter of sea water. The expression for dynamic topography is

$$\Delta Z = \int_{1130}^0 g^{-1}(\alpha - \alpha_0) dp \quad (3)$$

$\Delta Z$  is the height difference and  $\alpha$  is the specific volume.  $\alpha_0$  is the specific volume as a function of pressure but for a fixed temperature of 0°C and a salinity of 35 p.s.u. In Fig. 3 we see the dynamic topography anomaly which is the difference between the dynamic topography as given by Eq. (3) for the main experiment and the corresponding dynamic topography for tem-

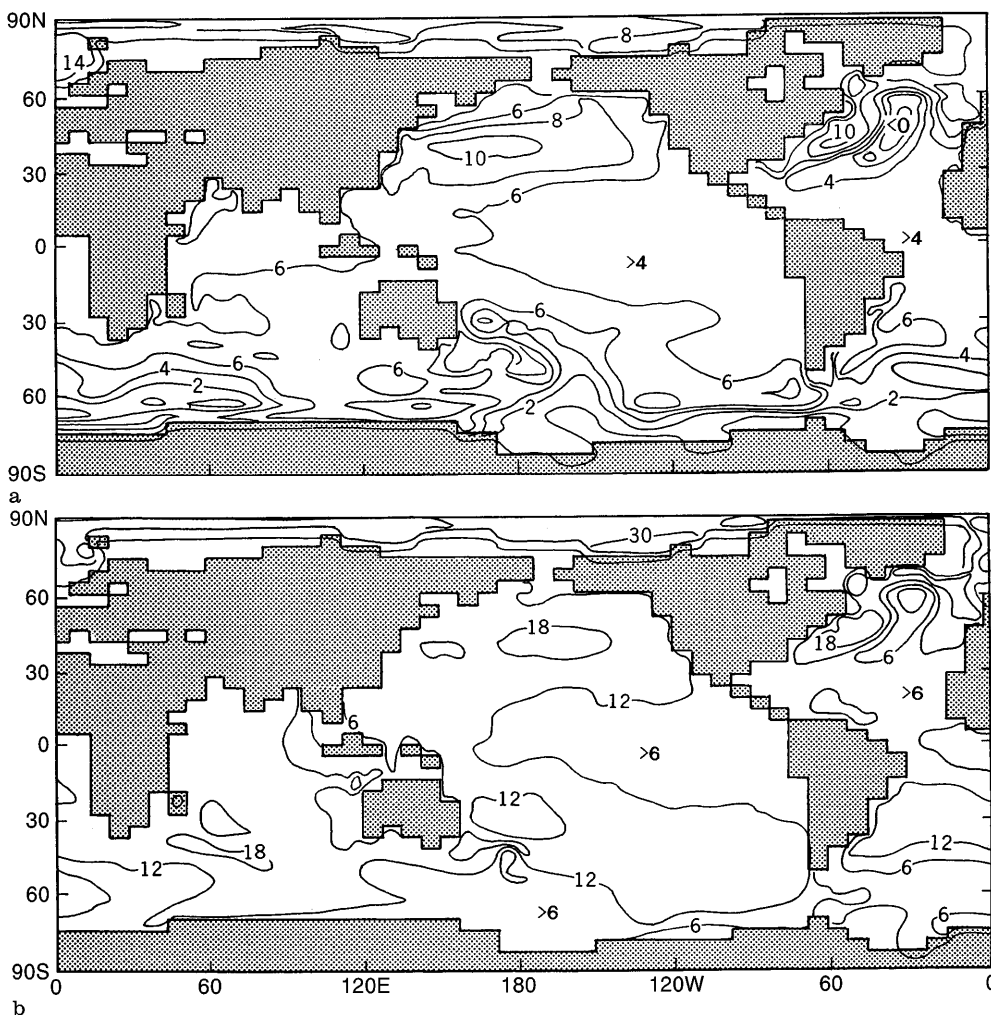


**Fig. 3a, b.** Global patterns of dynamic height rise (cm) associated with enhanced greenhouse warming in centimeters due to thermal expansion and changes in ocean circulation in the model. Assuming a 1% increase in atmospheric carbon dioxide starting in 1955, **a** corresponds to a decadal average centered on year 45, and **b** corresponds to a decadal average centered on year 75. Note that the addition of the historical trend of 10–20 centimeter rise per century would approximately double the net rise shown in this figure

perature and salinity corresponding to a 100 year average of the control run.

Figure 3 shows dynamic topography change defined above, and averaged over two separate ten-year periods. The initial greenhouse forcing of the model corresponds to the start of the Mauna Loa record in 1955. The experimental set up implicitly assumes that the ocean and atmosphere were in climate equilibrium at that time. Actually greenhouse forcing has been increasing since the start of the industrial age. For this and perhaps other unknown reasons global climate appeared to be drifting to a warmer state in 1955. The error involved in neglecting initial climate drift in an experiment of this type has been identified as a "cold start error". Estimates of this error have been attempted by Hasselmann et al. (1993). The two ten-year periods in Fig. 3 represent the averages of decades centered around 45 years and 75 after the start of the experiment. It must be kept in mind that the predicted rise in Fig. 3 includes only the thermal expansion due to projected greenhouse warming, neglecting the background rise due to other mechanisms, such as the growth or the shrinkage of land ice.

The decadal average sea level patterns shown in Fig. 3 allow some insight on the transient aspects of sea level rise due to the fact that the enhanced heating of the ocean is not globally uniform. In the decadal average pattern centered on year 45 shown in Fig. 3a we see that the sea level rise in the Southern Ocean is only 2–4 cm, while it is over 6 cm in many places north of the Circumpolar Current in the Pacific and Indian Oceans. In the earlier decade centered on year 45 there is a rather sharp gradient between the sea level rise around Antarctica and the zone just to the north. This gradient is still present in the later decadal average shown in Fig. 3b centered on year 75, but it is less pronounced. A feature common to both periods is a relative minimum rise in the eastern tropical Pacific. In the Northern Hemisphere ocean there are small areas in both the subpolar North Atlantic and North Pacific where the rise exceeds 8 cm. An interesting dipole pattern exists in the North Atlantic which is present in both patterns. The dipole pattern consists of a region of minimum rise just south of the axis of the Gulf Stream extension and a region of maximum rise just to the north. Note that the peak to peak amplitude of the dipole pattern is about 10 cm for the decade centered on year 45, and is about the same for the decade centered on year 75. For the first period the amplitude of the dipole is approximately equal to twice the average sea level rise. In Fig. 3b, the dipole intensity is slightly masked by the greater average rise. It should be noted that Delworth et al. (1993) note a similar dipole anomaly in dynamic topography in connection with a 4–5 decade time scale climate variability in the North Atlantic. However, the amplitude is only a few centimeters, indicating that the dipole in Fig. 3 is strong compared to natural variability of the model.

The main trend in the sea level patterns seems to be a decrease in relative intensity of the geographical variations in sea level rise as the temperature anomalies

penetrate to deeper and deeper levels where the horizontal gradients of density became much weaker. In later sections, we will address possible explanations for these striking regional variations of sea level rise shown in Fig. 3, which are particularly striking in the earlier stages.

A zonal average of Fig. 3b is shown in Fig. 4. The curve indicates a maximum in the ventilation around 40°N and 40°S. At these latitudes the wind-driven Ekman pumping drives surface waters downward and incorporates water into the main thermocline (Luyten et al. 1983). In the North Atlantic there is another local maximum of sea level change near 60°N where a great deal of deep water mass formation takes place in the Labrador and Greenland Seas. The pattern of major heat uptake in subpolar latitudes is similar to the uptake pattern of transient geochemical tracers (see IPCC 1990 for a review).

A second curve in Fig. 4 shows the zonally averaged dynamic eight change assuming a constant salinity of 35 p.s.u. In this case the peak at 40°N is much more pronounced, indicating that salinity plays an important role in redistributing the density anomaly associated with enhanced greenhouse warming in the North Atlantic in a more uniform manner. In the Arctic Ocean the difference between the dynamic height change and the constant salinity dynamic height anomaly shows that freshening of surface waters dominates the sea level change near the pole.

One of the most interesting features in Fig. 3 is the dipole pattern of sea level rise predicted by the model in the North Atlantic. I examine this feature in more detail in Fig. 5. Figure 5a, b shows the patterns of sea level and surface velocity averaged over years 70–80 of the enhanced greenhouse warming run. In Fig. 5a the sea level is estimated directly from the time-averaged velocity and wind field. Details are given in the Appendix. We see well developed subtropical and subarctic

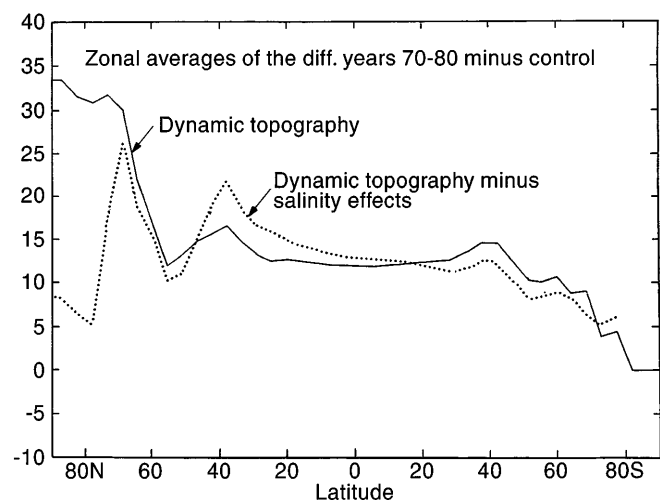


**Fig. 4.** Zonal averages of the sea level rise from dynamic topography (*solid*) and the dynamic topography difference (*dotted*) assuming a constant salinity of 35 p.s.u. The patterns corresponds in time to the decadal average centered on year 75 as in Fig. 3b

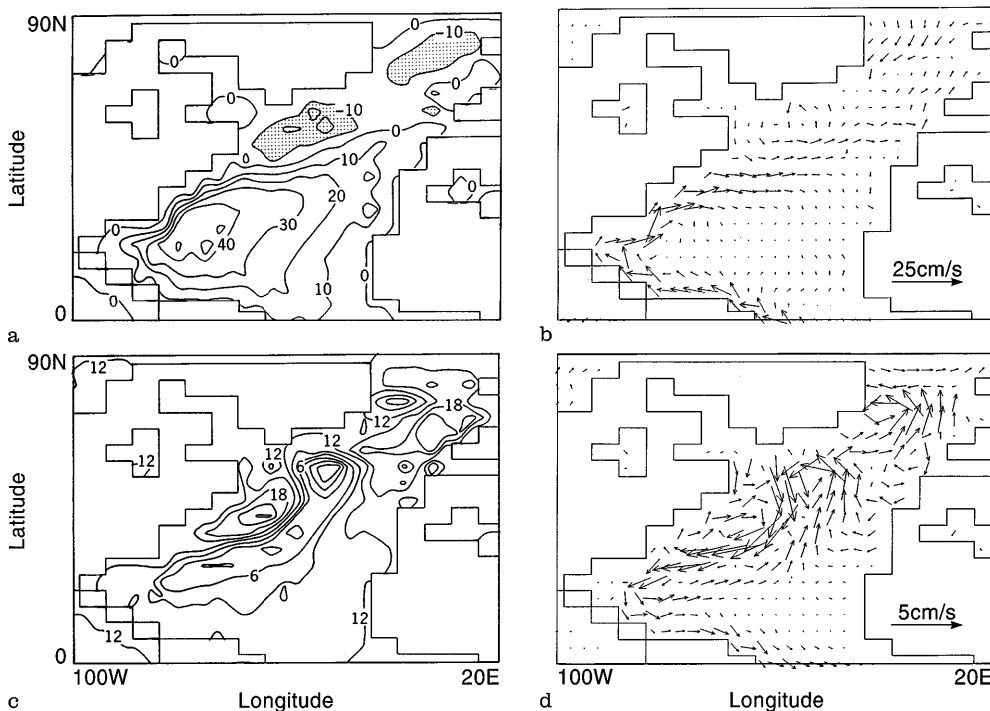


**Fig. 5a-d.** The North Atlantic dipole anomaly shown in greater detail. **a** The pattern of sea level calculated by the residual method based on an average of years 70–80. Details of the method are given in the Appendix. **b** Surface flow vectors corresponding to **a**. **c** The difference in surface elevation for the average of years 70–80 and the 100 year average of the control run. **d** The surface flow vectors corresponding to a weakening of the North Atlantic overturning

wind-driven gyres. The subtropical gyre has marked western intensification. The difference between the upper two figures and the 100 year average of the control run is shown in Fig. 5c, d. The vector differences, which are shown in Fig. 5d, show a marked weakening of poleward flow connecting the subtropical gyre to the subarctic gyre. Since changes in wind-stress patterns are rather minor, the pattern Fig. 5d is consistent with a weakening of the upper branch of the Atlantic thermohaline circulation as shown by Stouffer et al. (1989). Thus, the model suggests that once an allowance is made for changes in the wind-driven circulation, the sea level profile across the Gulf Stream should be a valuable indicator of a weakening of the Atlantic thermohaline circulation. We will return to this point in the conclusions.

#### 4 Tracor transport and spin-down

Omitting the effect of melting glaciers and ice caps, the sea level rise due to global warming is related to the addition of heat to the water column and its lateral redistribution. As a useful guide to understanding our results we consider the governing equation for heat in the ocean.  $\theta$  is the potential temperature and  $\mathbf{u}$  is the horizontal velocity vector associated with the large-scale circulation.  $Q$  is the effect of smaller scale, transient motions on the mixing of heat, and  $\nabla$  is the horizontal gradient operator. Let

$$\partial_t \theta' + (\bar{\mathbf{u}} + \mathbf{u}') \nabla (\bar{\theta} + \theta') + (\bar{w} + w') \partial_z (\bar{\theta} + \theta') = \bar{Q} + Q' \quad (4)$$

where the barred components are associated with the normal steady state ocean circulation and the primed

components are related to the perturbations caused by greenhouse warming. Subtracting the mean state, and neglecting higher order effects,

$$\partial_t \theta' = -\bar{\mathbf{u}} \nabla \theta' - \bar{w} \partial_z \theta' - \mathbf{u}' \nabla \bar{\theta} - w' \partial_z \bar{\theta} + Q' \quad (5)$$

The first and second term on the right hand side are the effects of the mean circulation advecting the heat anomalies. We will call this the “tracer” effect. The third and fourth term on the right hand side are the effect of perturbations on the ocean circulation acting on the mean temperature field. We will call this the “spin-down” effect, because enhanced greenhouse warming of the ocean in polar latitudes causes the thermohaline circulation to lose intensity.  $Q'$  on the right hand side represents remaining terms associated with possible changes in the level of transient mixing associated with greenhouse warming.

As noted in the previous section, the primary pathways of the ocean circulation connecting surface waters and deep water exist at high latitudes. Heat input as a function of latitude in the original experiment of Manabe et al. (1991) is shown in Fig. 6a. Note that most of the heat input takes place in the higher latitudes of the Southern Ocean, but there is also a sizable contribution from the high-latitudes of the Northern Hemisphere in spite of the small area of the northern oceans poleward of  $50^\circ\text{N}$ . Most of the Northern Hemisphere contribution comes from the North Atlantic, because the North Pacific does not extend above  $60^\circ\text{N}$ .

If the anomalous heat input due to enhanced greenhouse warming shown in Fig. 6a was not redistributed with respect to latitude, most of the sea level rise would be localized in the subpolar regions. Both the tracer term and the spin-down term in Fig. 6 smooth out sea level change by redistributing heat with respect

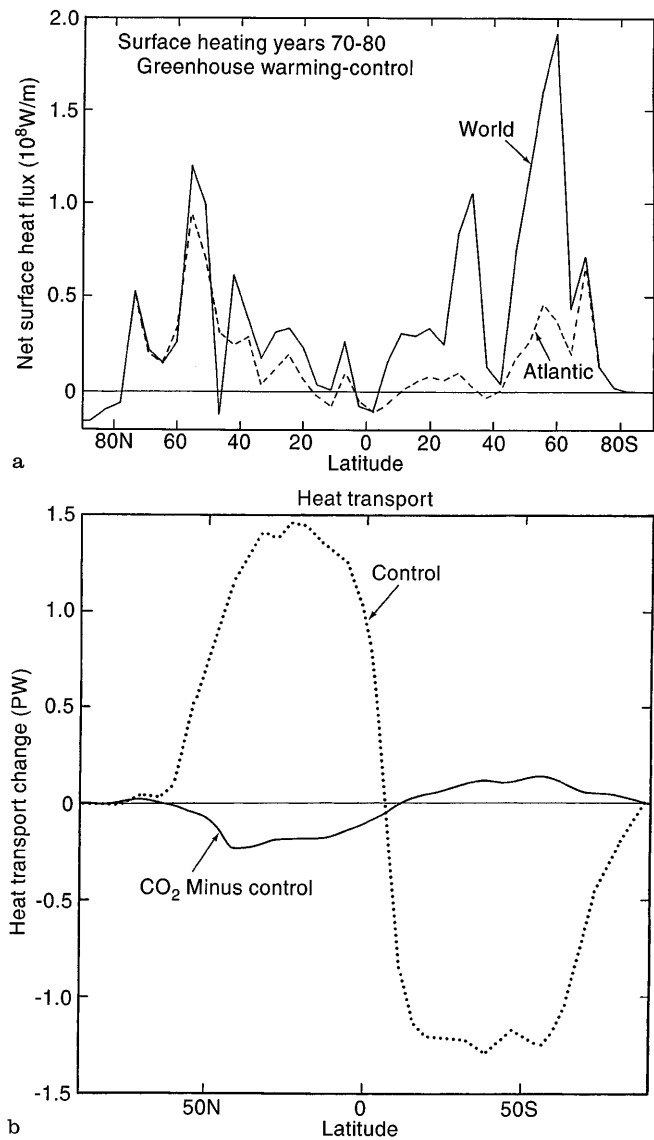


**Fig. 6.** **a** The excess heat flux received at the surface due to enhanced greenhouse warming, where years 70–80 of the control run were subtracted from the enhanced greenhouse run. The surface flux is integrated over the entire zonal belt and a span of 1 meter in the meridional direction. **b** The poleward transport of heat averaged over 100 years of the control run (*solid*) and the difference in poleward heat transport between the enhanced greenhouse warming run and the control run

to latitude. Figure 6b shows the northward transport of heat of the control run of Manabe et al. (1991) and the change in heat transport caused by enhanced greenhouse warming. The change reflects a spin-down of the thermohaline circulation and a consequent decrease in poleward heat transport due to the extra heat input at high latitudes shown in Fig. 6a. The reduction of poleward heat transport shown in Fig. 6b is about 0.1 PW or  $10^{14}$  W. A change in heat transport of this amount over a distance of one thousand kilometers or  $10^6$  m could give a divergence of heat of  $10^8$  W/m. This is the correct magnitude to balance the high subpolar input of heat shown in Fig. 6a. Hsieh and Bryan (1996) use a

very idealized model to examine how heat transport changes associated with such a spin-down of the thermohaline circulation can take place, and what time scales are involved.

## 5 The tracer effect

The advection of a temperature anomaly by the time-averaged ocean circulation is directly analogous to the advection of a passive tracer in the ocean. This process which corresponds to the first two terms on the right hand side of Eq. (5), has been extensively studied through modeling and the analysis of observations (see IPCC 1990, Ch. 1 for a recent review). The main sources of data are measurements of bomb-produced carbon-14, bomb-produced tritium, and chlorofluorocarbons produced by industry. These data show that tracers are spread rather rapidly in the upper thermocline on decadal time scales, but the lateral spread in deep waters is very slow (Toggweiler et al. 1989).

Fortunately, an idealized tracer experiment was carried out in conjunction with the revised calculations of greenhouse warming of this study. In this tracer calculation, the tracer was initially set to zero at all levels in the ocean. At the start of the integration the surface value of the tracer is fixed to unity and remains at that value throughout the 100 year integration. The tracer spreads from the surface down into the interior of the ocean. At time equal to infinity, we would expect that the tracer would reach a uniform value of unity throughout the volume of the ocean. The speed at which the tracer approaches such a uniform value in the interior of the ocean is a measure of the rate of mixing by the ocean circulation. A more ideal tracer experiment would consist of a linear build up of tracer at the upper boundary. Such an experiment would have been a closer analogue of greenhouse warming than a “switched on” tracer experiment. Nevertheless, the results shown in Fig. 7 are a valuable indicator of the tracer mechanism acting alone.

Zonally and vertically averaged values of the tracer are shown in Fig. 7 at various stages of the integration. It is obvious that the largest values are in the subpolar regions, which coincide with the location of the deep-water formation regions. As time goes on the tracer spreads into lower latitudes, but even by the decade 70–80, (corresponding to 2025–2035 AD) the tracer distribution is far from uniform. We interpret these results as evidence that the tracer term on the right hand side of Eq. (5) is not very effective in redistributing heat. If this term was acting alone, the sea level changes shown in Fig. 4 would be much less uniform than they are, and the largest rises would be concentrated in high latitudes.

## 6 Summary and conclusions

The expansion of the oceans due to global warming is a single component of global sea level rise. Although this component is much smaller than the potential con-

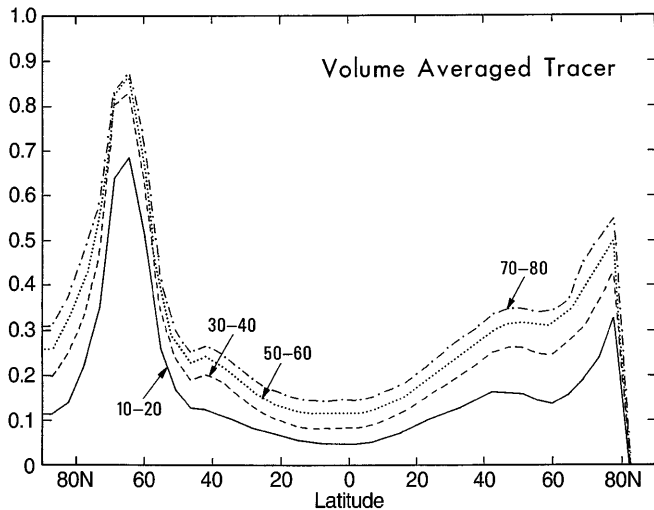


**Fig. 7.** Volume-averaged values of an idealized tracer as a function of latitude and time. The idealized tracer is initially zero everywhere in the ocean. In the experiment with the coupled model, the tracer is kept at a fixed value of unity at the ocean surface and allowed to spread downward surface and allowed to spread downward into the ocean interior

tribution of melting of major ice sheets, it is of great interest because it responds rapidly to changes in the global heat balance and is therefore a useful indicator. Measurements of sea level change coupled with a precise monitoring of ice sheets and glaciers provide a measure of how rapidly climate is changing.

This study is based on an analysis of the implied sea level changes in a coupled ocean-atmosphere model reported on by Stouffer et al. (1989) and Manabe et al. (1991). As pointed out by Douglas (1991), very little is known about the non-equilibrium aspects of sea level rise. The coupled ocean-atmosphere model includes most of the major factors in climate. Starting from an equilibrium state, atmospheric carbon dioxide is increased according to the "business as usual" scenario of the IPCC. The implied sea level changes in this integration were compared with a control integration in which atmospheric carbon dioxide is kept constant. Starting at 1955 AD, the "business as usual" scenario implies a doubling of atmospheric carbon dioxide by the year 2030 AD.

At year 75 the model, neglecting a "cold start error", predicts a rise in sea level by thermal expansion of  $15 \pm 5$  cm, which would imply only a doubling of the rate of sea level rise already noted in the historical record of the past century. The uncertainty of 5 cm is estimated by the "climate drift" in the sea level of the control run of the coupled model. Generally the predicted rise is greatest in the subpolar regions of both hemispheres where the enhanced heat input is greatest. There is an exceptionally large rise in the Arctic Ocean of the model, and exceptionally small rise near the Antarctic Continent. In the western part of the North Atlantic, there is an interesting dipole pattern associated with the weakening of the northward, surface

branch of the thermohaline circulation which connects the subtropical and subpolar gyres. The GFDL model predicts that the surface elevation gradient across the Gulf Stream should gradually weaken with respect to time with increased greenhouse warming. In fact, sea level records at Bermuda and Halifax, Nova Scotia suggest that the elevation gradient across the Gulf Stream has actually been increasing in the last two decades after a minimum in the early 1970s (Levitus 1990) at the time of the "great salinity anomaly". This suggests that natural variability in the North Atlantic circulation still dominates effects associated with potential greenhouse warming at the present time. Overall, many features of the coupled model agree with the results of the Max Planck Institute for Meteorology (Cubasch et al. 1992, 1994) and the British Meteorological Office Model (Gregory 1993). For the same greenhouse scenario, the overall rise is nearly the same, and even some of the regional features are similar. The lowest drift of the global sea level in the control run was obtained by Cubasch et al. (1992). This was only 2.5 cm compared to 5 cm in the present study and 12 cm in the Meteorological Office Study. The British Meteorological Office study indicates the dipole feature in the North Atlantic shown in Fig. 5, and also indicates a minimum rise around Antarctica. The Cubasch et al. (1992) study shows similar features in the sea level rise in the Southern Ocean as in the present study, including a maximum rise just to the north of the Antarctic Circumpolar Current. This feature was interpreted as evidence in a shift in position of the current. The dipole feature in the North Atlantic is not resolved in the Cubasch et al. (1992) study. Cubasch et al. (1994) carry out a very valuable series of Monte Carlo simulations and show that the calculated rise in global sea level are extremely robust to changes in the initial conditions, which helps to account for the very similar results obtained in all three coupled models.

An analysis of the model shows that most of the heat input takes place in the high-latitude zones, but there is a relatively uniform sea level rise at lower latitudes in both hemispheres. A linear analysis shows that small perturbations of heat can be redistributed with respect to latitude as a passive tracer by the time-averaged circulation, or by a weakening of the thermohaline circulation, a parallel "switch on" transient tracer experiment is carried out with the same coupled model which ordinarily transports heat from low- to high-latitudes. An analysis of the main experiment and the tracer experiment suggests that the weakening of poleward heat transport is the dominant mechanism for redistributing heat with respect to latitude, and that the tracer mechanism is rather weak.

An important question is whether a given pattern of sea level rise can be used as a "fingerprint" or indicator of enhanced greenhouse warming. Essentially the fingerprint concept requires a detailed knowledge of the sea level signals of natural variability, so that the proper discrimination can be made between the signature of natural variability and anthropogenically caused global change.

There are two puzzling features of the sea level rise predicted by the coarse resolution coupled ocean-atmosphere climate model of Manabe et al. (1991). One feature is the time scale of the ocean circulation spin-down, which weakens the normal poleward transport of heat. The signature of this effect in the sea level change solutions is a marked weakening of the slope of sea level across the Gulf Stream shown in Fig. 5. The second feature is the marked delay in sea level rise in the Southern Ocean in the immediate vicinity of Antarctica. The model predicts a slight increase in the geostrophic flow of the surface Antarctic Circumpolar Current. While these special features of the solution are very interesting in their own right they cannot be considered fingerprints of enhanced greenhouse warming without taking into account natural variability of the model, which appears to have the same sea level features with a smaller amplitude (Delworth et al. 1993). The simple, shallow water model provides studied by Hsieh and Bryan (submitted 1995) in a companion paper allows some insight on both of these features. It shows that the time scale of response is not controlled by the speed of coastal Kelvin waves, which rapidly transmit signals around the globe, but by a much slower process of transport in coastal jets which link high- and low-latitudes. Coastal jets cannot penetrate into the Southern Oceans south of Cape Horn, which may provide an explanation for the slow response of sea level in the extreme poleward parts of the Southern Ocean to buoyancy sources to the north. However, the wave response studied by Hsieh and Bryan (submitted 1995) cannot be the sole mechanism for redistributing buoyancy within the ocean. Advection and mixing must also play a significant role, particularly at critical points where the wave mechanism is least effective. The important role of rather narrow coastal currents in the redistribution of buoyancy in the simple model illustrates the need for continuing this type of study with higher resolution three-dimensional ocean models in future climate calculations.

*Acknowledgements.* The author is very grateful for the essential assistance received from R. J. Stouffer, K. Dixin and R. Pacanowski. Comments on a draft of the manuscript by R. J. Stouffer, K. Hamilton and V. Larcichev were very helpful. Reviews from J. Gregory and U. Mikolajewicz contributed to substantial improvements of the manuscript. The author is indebted to C. Raphael, J. Varanyak and A. Valerio for their assistance in preparing the figures and the manuscript.

## Appendix

Sea level is not an explicit variable in the GFDL ocean model (Bryan 1969). Therefore, it has to be computed diagnostically from the other variables, such as the velocity and wind stress field. Let  $\mathbf{u}$  be the horizontal surface velocity, and  $p$  be the surface pressure. The momentum equation for the horizontal velocity components in the surface layer is,

$$\nabla p = -\mathbf{G} + \mathbf{E} \quad (\text{A.1})$$

where  $\mathbf{G}$  represents

$$\mathbf{G} = \rho(\partial_t \mathbf{u} + \mathbf{u} \cdot \nabla \mathbf{u} + w \partial_z \mathbf{u} + f \mathbf{k} \times \mathbf{u}) - \mathbf{F} \quad (\text{A.2})$$

$\mathbf{F}$  is the horizontal stress exerted by small scale motions which cannot be resolved by the numerical grid, and  $\nabla$  is the horizontal gradient operator.  $\mathbf{E}$  is a small error vector, which is due to the fact that in the standard numerical implementation of the model there is a slight inconsistency between the way the coriolis forces are handled in the external relative to the internal mode. With a slightly more accurate formulation of the external mode, the error can be made to vanish within roundoff error, but this entails solving the external second order partial differential for the transport stream function with a nine point, rather than with the more compact five point laplacian star. In the case that  $\mathbf{E}$  vanishes, Eq. (A.1) can be integrated directly to find the surface pressure.

In the present case, Eq. (A.1) will not be exact in any case, since we are using time-averaged data and the non-linear terms in  $\mathbf{G}$  are neglected. Any error in Eq. (A.2), however, leads to inconsistent results when an attempt is made to solve for  $p$  by direct integration along different paths. To avoid this inconsistency, we adopt a variational approach which minimizes the error and provides a unique solution for the surface pressure field. The integral of the error variance over the whole upper layer of the World Ocean model is,

$$I = \iint (\nabla p + \mathbf{G})^2 a^2 \cos \phi \, d\phi \, d\lambda \quad (\text{A.3})$$

Minimizing  $I$ , we obtain

$$\nabla^2 p = -\nabla \cdot \mathbf{G} \quad (\text{A.4})$$

with the boundary condition consistent with no flow normal to the lateral boundaries.

$$\mathbf{n} \cdot (\nabla p + \mathbf{G}) = 0 \quad (\text{A.5})$$

where  $\mathbf{n}$  is a unit vector normal to the boundary. The calculation shown in Fig. 4a was done by applying Eq. (A.5) at interior points adjacent to the boundary. Equations (A.4) and (A.5) determine  $p$  within a global constant which is determined by the total volume of the ocean divided by the surface area.

## References

- Bryan K (1969) A numerical method for the study of the circulation of the World Ocean. *J Comput Phys* 4:347-376
- Bryan K (1984) Accelerating the convergence to equilibrium of ocean-atmosphere models. *J Phys Oceanogr* 14:666-673
- Bryan K, Komro FG, Rooth C (1984) The ocean's transient response to global surface temperature anomalies. In: *Climate processes and climate sensitivity*, Geophysical Monograph 29, Maurice Ewing 5, pp 29-38
- Bryan K, Manabe S, Spelman MJ (1988) Interhemispheric asymmetry in the transient response of a coupled response of a coupled ocean-atmospheric model to carbon-dioxide forcing. *J Phys Oceanogr* 18:851-867
- Cubasch U, Hasselmann K, Hoeck H, Maier-Reimer E, Mikolajewicz U, Santer BD, Sausen R (1992) Time-dependent greenhouse warming computations with a coupled ocean-atmosphere model *Clim Dyn* 8:55-69

- Cubasch U, Santer BD, Hellbach A, Hegerl GC, Hoeck H, Maier-Reimer E, Mikolajewicz U, Stoessel A, Voss R (1994) Monte Carlo climate change forecasts with a global coupled ocean-atmosphere model. *Clim Dyn* 10:1–19
- Cubasch U, Hegerl GC, Hellbach A, Hoeck H, Mikolajewicz U, Santer BD, Voss R (1995) A climate change simulation starting from 1935. *Clim Dyn* 11:71–84
- Crank J (1975) *The mathematics of diffusion* 2nd Ed. Clarendon Press, Oxford, UK
- Delworth T, Manabe S, Stouffer RJ (1993) Interdecadal variations of the thermohaline circulation in a coupled ocean-atmosphere model. *J Clim* 6:1993–2011
- Dobson F, Bretherton FP, Burridge DM, Crease J, Kraus EB, Vonder Haar TH (1982) The “cage experiment: a feasibility study. World Climate Programm, Ref. 22, World Climate Research Program, World Meteorological Organization, Geneva, Switzerland
- Douglas B (1991) Global sea level rise. *J Geophys Res* 96(C4):6981–6992
- Gornitz V, Lebedeff S (1987) Global sea level changes during the past century. In: Nummedal D, Pilkey OH, Howard JD (eds) *Sea-level fluctuation and coastal evolution*. SEPM Spec Publ 41
- Gornitz V, Lebedeff S, Hansen J (1982) Global sea level trends in the past century. *Science* 215:1611–1614
- Greatbatch RJ (1994) A note on the representation of steric sea level in models that conserve volume rather than mass. *J Geophys Res* 99:12767–12771
- Gregory JM (1993) Sea level changes under increasing anthropogenic CO<sub>2</sub> in a transient coupled ocean-atmosphere GCM experiment. *J Clim* 6:2247–2262
- Hasselmann K, Sausen R, Maier-Reimer E, Voss R (1993) On the cold start problem with coupled atmosphere-ocean models. *Clim Dyn* 9:53–61
- Hsieh WW, Bryan K (1996) The steric component of sea level rise associated with enhanced greenhouse warming: a simple model study. *Clim Dyn* (accepted)
- IPCC (1990) *Climate change: The IPCC assessment*. Houghton JT, Jenkins GJ, Ephraums JJ (eds) Cambridge University Press, Cambridge, UK
- Levitus S (1990) Interpentadal variability of steric sea level and geopotential thickness of the North Atlantic, 1970–1974 versus 1955–1959. *J Geophys Res* 95:5233–5238
- Luyten JR, Pedlosky J, Stommel H (1983) The ventilated thermocline. *J Phys Oceanogr* 13:292–309
- Manabe S, Stouffer RJ (1988) Two stable equilibria of a coupled ocean-atmosphere model. *J Clim* 1:841–866
- Manabe S, Stouffer RJ, Spelman M, Bryan K (1991) Transient responses of a coupled ocean-atmosphere model to gradual changes of atmospheric carbon-dioxide, Part I: annual mean response. *J Clim* 4:785–818
- Meier MF (1984) Contribution of small glaciers to global sea level. *Science* 226:1418–1421
- Mikolajewicz U, Santer BD, Maier-Reimer E (1990) Ocean response to greenhouse warming. *Nature* 345:589–593
- Munk W, Forbes AMG (1989) Global ocean warming: an acoustic measure. *J Phys Oceanogr* 19:1765–1778
- Peltier WR, Tushingham AM (1989) Global sea level rise and the greenhouse effect: might they be connected? *Science* 244:806–810
- Sausen R, Barthel K, Hasselmann K (1988) Coupled ocean-atmosphere models with flux correction. *Clim Dyn* 2:145–156
- Stouffer R, Manabe S, Bryan K (1989) Interhemispheric asymmetry in climate response to a gradual increase of atmospheric CO<sub>2</sub>. *Nature* 392:660–662
- Toggweiler JR, Dixon K, Bryan K (1989) Simulations of radiocarbon in a coarse resolution World Ocean model. II: distributions of bomb-produced <sup>14</sup>C. *J Geophys Res* 94:8243–8264
- Warrick R, Oerlemans J (1990) Sea level rise. In: Houghton JT, Jenkins GJ, Ephraums JJ (eds) *Climate Change: the IPCC Assessment*, Cambridge University Press, Cambridge, UK pp 261–279